(4)

Reprinted from the *Soil Science Society of America Proceedings*
Volume 36, no. 5, September-October 1972
677 South Segoe Rd., Madison, Wis. 53711 USA

Water Transmission Properties of an Asphalt Barrier[1]

J. P. PALTA, G. R. BLAKE, AND D. A. FARRELL[2]

ABSTRACT

The water transmission properties of an asphalt barrier were studied using samples taken from a barrier formed in Zimmerman fine sand. Steady flow experiments using a 9.0-cm diameter soil column showed that water movement through the barrier was affected by the capillary potentials on both sides of the barrier if these potentials exceeded a critical value or 'break point' which ranged from –32 to –20 cm depending on the flow rate. When the potential below the barrier dropped below the critical value, the potential above the barrier remained relatively unchanged. This steady value increased from –4.3 to –1.5 cm when the flow rate was increased from 0.009 to 0.058 cm/hour. The hysteretic flow properties of the barrier are explained using a model based on the following assumptions: (i) flow occurs mainly through cracks of varying width, and (ii) the ratio of the draining to wetting potentials of the cracks exceeds unity and is independent of crack size.

Additional Index Word: **soil discontinuities, steady state flow.**

THE PROFITABLE USE of sandy soils for agricultural purposes is often limited by their low water holding capacity. Such soils need to be irrigated frequently but the rapid percolation of water renders surface methods of irrigation impractical or inefficient. Because many sandy soils are otherwise well suited to profitable farming, several techniques for reducing deep percolation by the placement of relatively impermeable barriers within the soil have been suggested (Miller and Bunger, 1963; Erickson et al., 1968a).

The most reliable and the most widely used technique is the in situ placement of a continuous asphalt barrier using a hot liquid asphalt spray. With this technique asphalt barriers can be formed to soil depths of 60 cm. Hammond et al. (1967) found that a well-formed 3-mm thick asphalt barrier reduced the final infiltration rate for a deep sandy soil from 18.25 to 1.73 cm/hr. Erickson et al. (1968a) reported a 100% increase in the water holding capacity of a sandy soil due to the presence of an asphalt barrier. In another study Erickson et al. (1968b) found that 4 days after irrigation the soil water suction at the barrier soil interface was 11 cm H_2O whereas the suction at the same depth in the control plot had increased to 66 cm H_2O.

Significant increases in yield for various vegetable crops have also been reported (Erickson et al., 1968b; Hansen and Erickson, 1969; Saxena et al., 1968, and 1971). These increases are generally attributed to an increase in water storage above the barrier with the improved nutrient status of the soil being a secondary factor.

No attempt appears to have been made to determine the water transmission properties of asphalt barriers either in the field or in the laboratory. Because the field performance of these barriers cannot be analyzed for a range of surface flux conditions without this information, the work reported herein was undertaken to determine and, if possible, characterize those properties of the barrier that influence water movement.

MATERIALS AND METHODS

A continuous asphalt barrier was formed at a depth of 56 cm in Zimmerman fine sand by overlapping 225-cm wide strips. A spray of hot asphalt emulsion applied at a rate of 14,000 liters/ha produced an asphalt-sand layer 2 to 3-mm deep. Details of the technique and the machinery used in the field operation have been described by Hansen and Erickson (1969).

The transmission properties of a barrier were measured on undisturbed barrier samples taken from these field plots. A line diagram of the apparatus used in the laboratory study is shown in Fig. 1. The barrier sample was placed on a 1.5-cm layer of Zimmerman fine sand on a suction plate. In a 9-cm diameter plastic cylinder standing on top of the barrier, the same soil was packed uniformly to a height of 5 cm.

Three tensiometers were embedded into the soil, one 0.5 cm below, one 0.5 cm above, and one 4 cm above the barrier. The tensiometer cups were 1 cm diameter and 3 cm long. Two openings in the cup allowed for flushing, one of them being shut with a clamp, the other connected to a manometer filled with Meriam no. D-8325 indicating fluid (sp. gr. 1.74 g/cm^3) for measuring suctions (Trade names and company names are included for the benefit of the reader and do not imply any endorsement or preferential treatment of the product listed by the US Dep. of Agr. or the Univ. of Minn.). Manometers were connected to tensiometers using Temflex 105-extruded size 17 vinyl tubing. There was no observed hysteresis in the connecting tubes, and the capillary effect was less than 0.1-mm water pressure. Capillary potentials could be measured with a sensitivity of approximately 0.5-mm of water pressure.

A constant flow rate of water was maintained at the top of the cylinder, by use of a capillary tube resistance fixed between a Mariotte flask reservoir and a drawn glass dropper. Different flow rates were obtained by changing the height of the Mariotte flask. The number of drops per unit time falling on top of the soil surface was recorded and converted to centimeters of

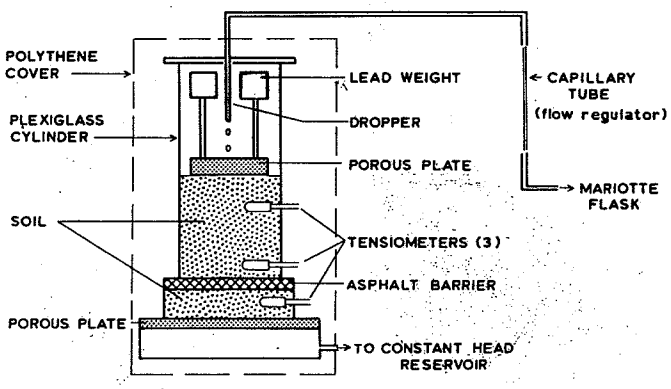

Fig. 1—Schematic diagram of apparatus used for steady state experiments.

[1] Contribution from the Dep. of Soil Science, Univ. of Minnesota, in cooperation with the Corn Belt Branch, Soil and Water Conservation Res. Div., ARS, USDA, St. Paul, Minnesota. 55101. Paper no. 7890, Scientific Journal Series. This investigation was supported in part by funds provided by the US Dep. of Interior, Office of Water Resour. Res. under act of 1964, P.L. 88-369. Presented before Div. S-1, Soil Science Society of America at New York, August 17, 1971. Received March 21, 1972. Approved June 9, 1972.

[2] Research Assistant, Professor, Univ. of Minnesota; and Soil Scientist, ARS, USDA, and Professor, Univ. of Minnesota, respectively, St. Paul.

water per unit area per unit time. With this system flow rate could be maintained nearly constant (variation of ± 4%) during 5 days of continuous operation.

Suction below the barrier was regulated by changing the height of the constant head reservoir. Water was allowed to enter the surface of the soil uniformly over its area by allowing the drops to fall on a porous plate at the top of the cylinder. In order to insure a good barrier-soil contact and to simulate overburden pressure in the field, a 6.8-kg weight was placed on the soil surface as shown in Fig. 1. For a wet bulk density of 1.9 g/cm^3 a weight of 6.81 kg is equivalent to an overburden of 56 cm of soil.

RESULTS

A typical relationship between soil water potential above (ψ_a) and potential below (ψ_b) a barrier, is shown in Fig. 2. The results infer relatively high conductivity of the barrier until ψ_b reaches a value of approximately 35 cm of water suction. At smaller values of ψ_b, i.e., higher suctions, the conductivity of the barrier decreases abruptly. At this stage ψ_a increases because water collects on top of the barrier. The sudden decrease in conductivity is associated with drainage of many of the cracks and fractures in the barrier. With further decrease in ψ_b from —35 to —82 cm, ψ_a remains relatively unchanged. With subsequent increase in ψ_b the barrier exhibits marked hysteresis.

Each point in Fig. 2 represents one set of equilibrium readings of ψ_a and ψ_b. To achieve each set of readings a known value of ψ_b was selected by regulating the height in the constant head reservoir (Fig. 1), and changes in ψ_a with time were recorded. An example of this is shown in Fig. 3 where capillary potentials ψ_a and ψ_b are plotted as functions of time. A steady state was assumed to have been reached when the difference in potentials (ψ_a — ψ_b) remained constant for 1 hour. As is clear from Fig. 3 steady state was normally reached in 3 to 5 hours. This was true for the ψ_b increasing curve and part of the ψ_b decreasing curve in Fig. 2, i.e. when ψ_a and ψ_b were changing in the same direction.

However, for the range in ψ_b where ψ_a increased as ψ_b decreased (Fig. 2) a period of several days was required for a steady state to be established. This is shown in Fig. 4.

With a flow rate of 0.2 cm/hour when the suction below the barrier was increased from 33.5 to 41.6-cm, about 124 hours were required for ψ_a to increase from the initial value of 32.3 cm to the equilibrium value of 5.6-cm suction. Equilibration time, however, will depend upon the capacity of the system to take up water (pore volume) and the flow rate. In general, the lower the flow rate and the higher the pore volume, the longer will be the time required to reach a steady state. The oscillations in the capillary potential above the barrier shown in Fig. 4 are interpreted as indicating an instability in the system.

The steady flow experiment was repeated with another sample of barrier for different flow rates. The results are shown in Fig. 5. It is clear that the minimum value of ψ_a, hereafter called the break point, is largely dependent on the flow rate. When the flow rate was increased from 0.009 cm/hour to 0.058 cm/hour, the break point increased from ψ_a = —32 to —20-cm of water. A similar pattern was obtained for maximum ψ_a reached at minimum ψ_b. This value was —4.3 at a flow rate of 0.009 cm/hour and —1.5 cm at a flow rate of 0.058 cm/hour. In general for any value of ψ_b the value of ψ_a increased with increase in flow rate.

DISCUSSION

A principal objective of this study was to establish whether or not the transmission properties of an asphalt barrier were comparable to those of soils or other granular porous materials. If the barrier is comparable to a layer of granular material of finite thickness L and if the effects of the gravitational and osmotic components of the potential

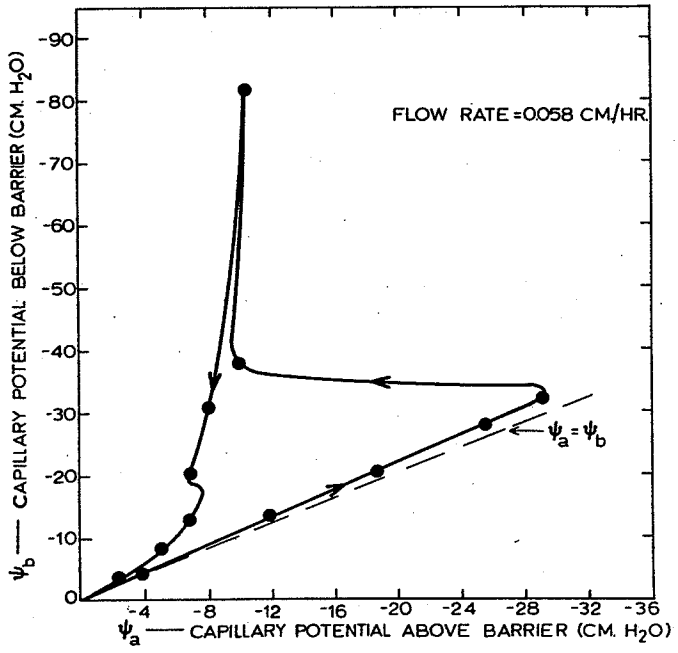

Fig. 2—Observed relationship between soil water potentials above and below an asphalt barrier.

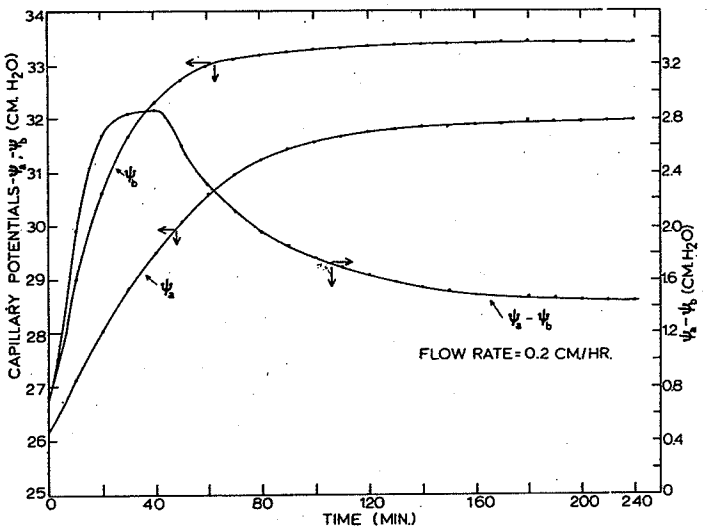

Fig. 3—Changes in soil water potentials above and below an asphalt barrier, ψ_a and ψ_b, with time for a steady state experiment.

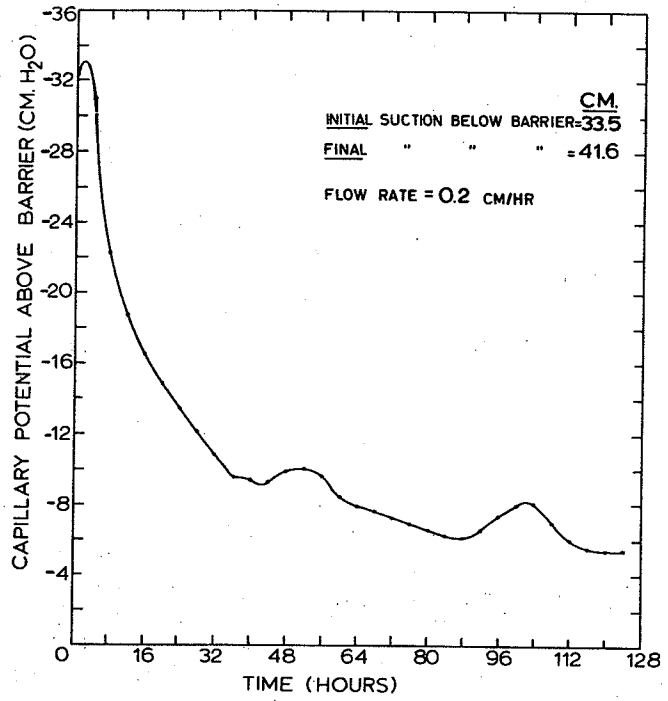

Fig. 4—Changes in water potential above an asphalt barrier, ψ_a, with time at the break point for a steady state experiment.

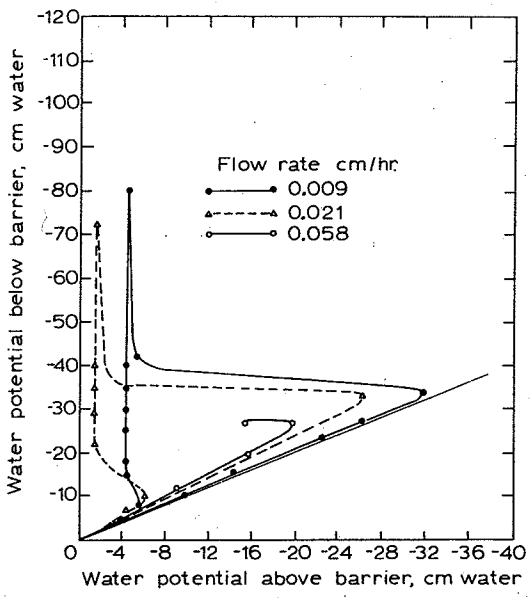

Fig. 5—Observed relationship between soil water potentials above and below an asphalt barrier, ψ_a and ψ_b at various flow rates.

are neglected, we can readily derive an equation describing the capillary potential profile for steady flow through the barrier. Steady one-dimensional flow of water through a uniform granular porous medium is given by

$$q = -K(\partial\Phi/\partial x) \qquad [1]$$

where q is the flow rate, K is the hydraulic conductivity (normally a function of the water content), Φ is the total macroscopic potential of the water at a point in the medium, and x is the spatial co-ordinate taken positive in the direction of flow. For vertical flow Φ has capillary, osmotic, and gravitational components. Neglecting the osmotic component and limiting our treatment to the case where the capillary potential gradients greatly exceed the gravitational gradient, equation [1] may be written as

$$q = -K(\partial\psi/\partial x) \qquad [2]$$

where ψ is the capillary potential. The gravitational potential could easily be included in the analysis, but since it does not effect the conclusions, it was omitted. If flow through an asphalt barrier is comparable to flow through a granular porous medium, with K and ψ continuous functions of the water content, then

$$qL = \int_{\psi_b}^{\psi_a} K d\psi \qquad [3]$$

where L is the thickness of the barrier and ψ_a and ψ_b are the capillary potentials at the upper and lower soil-barrier interfaces, respectively. It follows from [3] that for constant q, changes in ψ_a and ψ_b will be in the same direction. This is shown in Fig. 6 where it is clear that for a typical porous medium for constant flow rate, ψ_a decreases as ψ_b decreases. The results of the laboratory experiments (Fig. 2 and Fig. 5) indicate that for constant flow through an asphalt barrier, the measured relationship between ψ_a and ψ_b is inconsistent with the relationship for a granular medium. For the asphalt barrier at selected ranges of ψ_b, ψ_a increases as ψ_b decreases and ψ_a decreases as ψ_b increases as noted in Fig. 6.

In view of the hysteretic nature of water transmission properties of asphalt barriers, adequate characterization of these properties by experiment presents a formidable task. Physical models which permit the transmission properties of the barrier to be predicted from more limited experimental information need to be developed. The following model exhibits many of the observed characteristics of an asphalt barrier and lends itself to further development. For our proposed model, flow through the barrier is assumed to

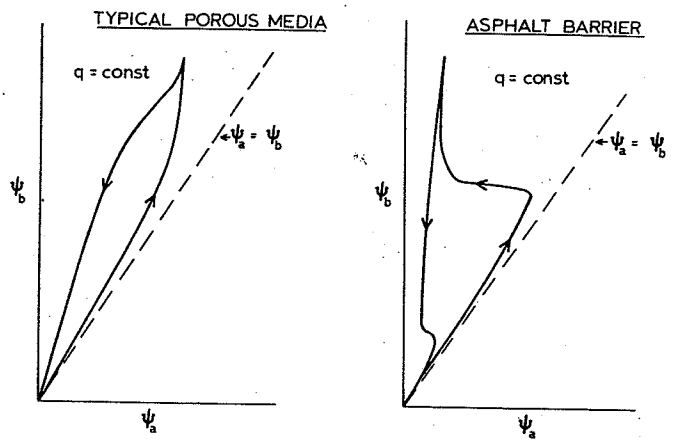

Fig. 6—Postulated soil water potentials at two elevations, ψ_a and ψ_b, in typical porous media and in the same with an asphalt barrier separating the two measuring points.

occur mainly through cracks of various sizes. A difference between the wetting and draining potentials for a crack is assumed to give rise to the hysteretic flow properties of the barrier. The model allows for possible movement of additional water through soil-filled cracks. The transmission properties of these cracks are assumed to be similar to those of a granular material.

The model assumes that the conductivity per unit area K_i of any crack having a draining potential ψ_i is related by

$$K_i = A\psi_i^{-2} \qquad [4]$$

where A is a constant independent of ψ_i. If the width, $2r_i$ of a planar crack is assumed uniform and if the length of the crack and the thickness of the asphalt barrier are substantially greater than $2r_i$ the conductivity, K_i, of the crack may be expressed as

$$K_i = r_i^2/3\mu \qquad [5]$$

where μ is the viscosity of water. The draining potential ψ_i of this planar crack is related to r_i by

$$\psi_i = \sigma \cos \beta / r_i \qquad [6]$$

where σ is the surface tension of water and β is the contact angle for a receding meniscus. Combining equations [5] and [6] gives

$$K_i = \psi_i^{-2} [\sigma^2 \cos^2 \beta / 3\mu]. \qquad [7]$$

It is clear that equation [7] is a specific form of equation [4]. However the cracks in a barrier will not usually have the simple geometry used to obtain equation [7]. Consequently, the more general expression given by equation [4] which remains valid provided all the cracks have the same geometry is preferred. The model also assumes that the wetting potential of the crack ψ_w is proportional to the draining potential of the crack, ψ_d. This may be written as

$$\psi_w = \gamma \psi_d \qquad [8]$$

where γ is another constant, also independent of ψ_i.

At any given ψ_a and ψ_b under steady state conditions, some of the cracks will be filled with water, others will remain empty, still others may contain some water pockets and some empty space, creating a zone of hydraulic resistance at the lower barrier-soil interface. For decreasing ψ_b, the cracks that remain filled with water have a draining potential less than ψ_b; cracks that remain empty have a draining potential greater than ψ_a during a draining cycle, and a wetting potential greater than ψ_a during the wetting cycle. The remaining cracks with draining potential greater than ψ_b and less than ψ_a are assumed to develop a zone of hydraulic resistance at the barrier-soil interface. Hence the resultant steady state-flow will be through these three types of cracks. The contribution of the water-filled cracks to the flow rate is given by

$$q' = A [\psi_a - \psi_b] \sum_{i=b}^{n} \psi_i^{-2} \qquad [9]$$

where ψ_a-ψ_b is the potential difference and $A\ \psi_i^{-2}$ is the conductance from equation [4]. The contribution of the soil-filled cracks of the flow rate is deduced from [3] as

$$q'' = \mathrm{L}^{-1} \int_{\psi_b}^{\psi_a} K_s(\psi)\, d\psi. \qquad [10]$$

The contribution of the cracks that develop a zone of hydraulic resistance at the barrier-soil interface is given by

$$q''' = A \sum_{i=1}^{b} [\psi_a - \psi_i \gamma]\, \psi_i^{-2}. \qquad [11]$$

In this case the potential difference is $\psi_a - \gamma\psi_i$ and not $\psi_a - \psi_b$ as in equation [9], $\gamma\psi_i$ being the wetting potential of the crack. The use of $\psi_a - \psi_i$ is also justifiable, but when ψ_i is used instead of $\gamma\psi_i$ the predicted curve does not follow the experimental curve. The true potential at the bottom of the crack will be somewhere in between ψ_i and $\gamma\psi_i$ because the crack does not drain fully and then rewet. This was confirmed from observations on flow through a simulated crack (by putting two pieces of plastic sheet at a distance of ⅓ mm).

From equations [9], [10], and [11] we can write the total flow q as the sum of the individual flows.

$$q = q' + q'' + q'''. \qquad [12]$$

To illustrate the behavior of the proposed model, we assume that the crack size distribution is given as

$$\psi = \psi_o \exp[\alpha(\theta_o - \theta)] \qquad 0 \leqslant \theta \leqslant \theta_o. \qquad [13]$$

Now for any arbitrarily selected γ we can determine a relationship between ψ_a and ψ_b in terms of the flow rate and the parameters α and θ_o. In equation (13) ψ_o is the draining potential of the largest crack, θ_o is the fractional surface area of the barrier that transmits water at a potential ψ_o, θ is the fractional surface area that conducts water at a potential ψ, and α is a crack distribution parameter. For a given θ_o a large value of α indicates a wide range in crack size and a small value of α indicates a narrow range in crack size.

If the soil water potential ψ_b below the barrier is greater than ψ_o the draining potential of the largest crack, then all the cracks conduct water and from equation [9] we get

$$q' = A [\psi_a - \psi_b] \int_{\theta(\psi_m)}^{\theta(\psi_o)} \psi^{-2}(\theta)\, d\theta \qquad [14]$$

where $\psi_m = \psi_o \exp(\alpha\theta_o)$ is the potential of smallest crack and $q''' = 0$.

If $\psi_m < \psi_b < \psi_o$ then only cracks completely filled with water contribute to q' and we get

$$q' = A\,[\psi_a - \psi_b] \int_{\theta(\psi_m)}^{\theta(\psi_b)} \psi^{-2}(\theta)\,\theta d. \qquad [15]$$

If $\psi_a < \psi_b$ and $\psi_b < \psi_o$ then cracks in the barrier will either be nonconducting or their contribution to the flow rate will be included in q', and $q''' = 0$.

If ψ_b is less than ψ_o, ψ_a is greater than $\gamma\psi_b$ and ψ_a is greater than or equal to $\gamma\psi_o$ then from equation [11]

$$q''' = A\,\psi_a \int_{\theta(\psi_b)}^{\theta(\psi_o)} \psi^{-2}(\theta)\,a\theta \; - A\gamma \int_{\theta(\psi_b)}^{\theta(\psi_o)} \psi^{-1}(\theta)\,d\theta \qquad [16]$$

giving $q' + q'''$ = equation [15] + equation [16] [17]

If ψ_b is less than ψ_o and ψ_a is greater than $\gamma\psi_b$ but less than $\gamma\psi_o$ then from equation [17]

$$q''' = A\,\psi_a \int_{\theta(\psi_b)}^{\theta(\psi_a/\gamma)} \psi^{-2}(\theta)\,d\theta \; - A\gamma \int_{\theta(\psi_b)}^{\theta(\psi_a/\gamma)} \psi^{-1}(\theta)\,d\theta \qquad [18]$$

giving $q' + q'''$ = equation [15] + equation [18] [19]

Substituting for $\psi(\theta)$ from equation [13] in equations [14], [15], [17], and [19] gives after integration

$$q' + q''' = \frac{A}{2\alpha}(\psi_a - \psi_b)\left(\frac{1}{\psi_b^2} - \frac{1}{\psi_m^2}\right) \qquad [20]$$

$$q' + q''' = \frac{A}{2\alpha}(\psi_a - \psi_b)\left(\frac{1}{\psi_b^2} - \frac{1}{\psi_m^2}\right) \qquad [21]$$

$$q' + q''' = \frac{A}{2\alpha}(\psi_a - \psi_b)\left(\frac{1}{\psi_b^2} - \frac{1}{\psi_m^2}\right) + \frac{A}{2\alpha}(\psi_a)\left(\frac{1}{\psi_o^2} - \frac{1}{\psi_b^2}\right) - \frac{A\gamma}{\alpha}\left(\frac{1}{\psi_o} - \frac{1}{\psi_b}\right) \qquad [22]$$

$$q' + q''' = \frac{A}{2\alpha}(\psi_a - \psi_b)\left(\frac{1}{\psi_o^2} - \frac{1}{\psi_m^2}\right) + \frac{A}{2\alpha}(\psi_a)\left(\frac{\gamma^2}{\psi_a^2} - \frac{1}{\psi_b^2}\right) - \left(\frac{A\gamma}{\alpha}\right)\left(\frac{\gamma}{\psi_a} - \frac{1}{\psi_b}\right). \qquad [23]$$

For ease of presentation ψ_a and ψ_b have been normalized by dividing them by ψ_m, the draining potential of the smallest crack in the crack size distribution. In addition a generalized flow rate q^* is used with the relationship between q^* and $q' + q'''$ given by the expression.

$$q^* = (2\alpha\psi_m/A)\,(q' + q'''). \qquad [24]$$

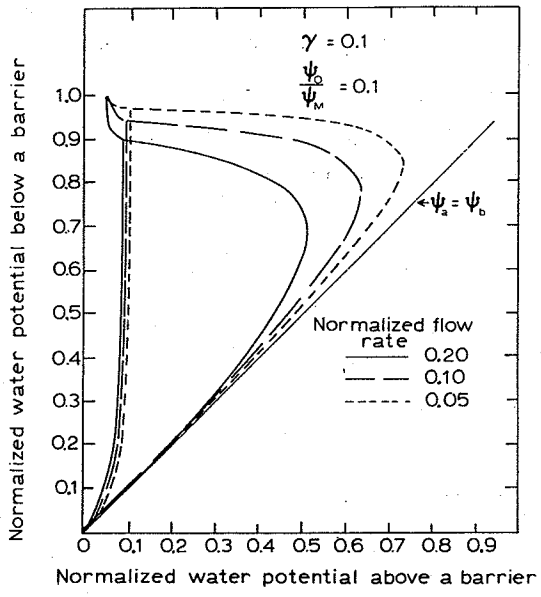

Fig. 7—Model-predicted relationship between normalized soil water potentials above and below an asphalt barrier, ψ_a^* and ψ_b^*, where $\gamma = 0.1$.

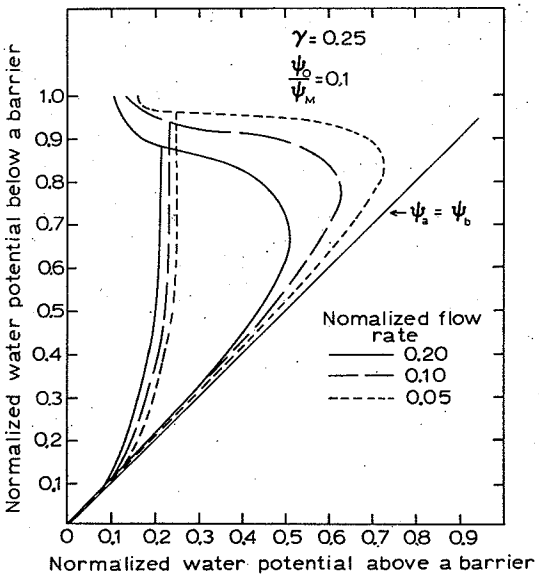

Fig. 8—Model-predicted relationship between normalized soil water potentials above and below an asphalt barrier, ψ_a^* and ψ_b^*, where $\gamma = 0.25$.

Using this model the relationship between ψ_a^* and ψ_b^* for selected values of q^*, $(\psi_o/\psi_m) = 0.1$ and $\gamma = 0.1$ and 0.25 have been computed and shown in Fig. 7 and Fig. 8. (The calculations were made on a computer and the program will be made available on request). It is evident from these figures that the behavior of the proposed model closely resembles that of the barrier (Fig. 2). The hysteretic characteristics of the model shown in Fig. 7 and Fig. 8 are obtained by assuming that the barrier is completely saturated with water for decreasing ψ_b while some of the cracks are empty and nonconducting for increasing ψ_b.

As we might expect Fig. 7 and Fig. 8 show that a de-

crease in γ lowers the suction at the top of the barrier, at which drainage through the barrier will occur. A nonwetting barrier should insure that the water conservation above the barrier will be maintained at high level at all times. The drainage characteristics of the barrier will be determined primarily by the crack distribution and are not significantly influenced by γ.

LITERATURE CITED

1. Erickson, A. E., C. M. Hansen, and A. J. M. Smucker. 1968a. The influence of subsurface asphalt barriers on the water properties and the productivity of sand soils. Int. Congr. Soil Sci., Trans. 9th (Adelaide, Aust.) I:331–337.
2. Erickson, A. E., C. M. Hansen, A. J. Smucker, K. Y. Li, L. C. Hsi, T. S. Wang, and R. L. Cook. 1968b. Subsurface asphalt barriers for the improvement of sugarcane production and the conservation of water on sand soil. Int. Soc. Sugar Cane Technologists, Proc., 13th Congr., Taiwan, 787–792.
3. Hammond, L. C., H. W. Lundy, and G. K. Saxena. 1967. Influence of underground asphalt barriers on water retention and movement in Lakeland fine sand. Soil Crop Sci. Soc. Fla., Proc. 27:11–19.
4. Hansen, C. M., and A. E., Erickson. 1969. Use of asphalt to increase water holding capacity of droughty sand soils. Ind. Eng. Chem. Prod. Res. Develop. 8:256–259.
5. Miller, D. E., and W. C. Bunger. 1963. Moisture retention by soil with coarse layer in the profile. Soil Sci. Soc. Amer. Proc. 27:586–589.
6. Saxena, G. K., L. C. Hammond, and H. W. Lundy. 1968. Effect of an asphalt barrier on soil salinity and yield of vegetables under variable irrigation and fertilization. Soil Crop Sci. Soc. Fla., Proc. 28:310–318.
7. Saxena, G. K., L. C. Hammond, and H. W. Lundy. 1971. Effect of an asphalt barrier on soil salinty and yields and water use by tomato and cabbage. J. Amer. Soc. Hort. Sci. 96:218–222.